Journal of Civil Engineering and Materials Application

Journal home page: http://jcema.com

Received: 17 February 2022 • Accepted: 30 March 2022

Research

doi: 10.22034/jcema.2022.149988

Evaluation of Effect of Force Generated in Bolts with T-stub Connections

Lisa Hanumm, Wang Han*

Department of Civil engineering, School OF Civil Engineering and Transportation, Beijing, China.

*Correspondence should be addressed to Wang Han, Department of Civil Engineering, School of Civil Engineering and Transportation, Beijing, China. Tel: +86 10 6327 6501; Fax: +86 10 6327 6501; Email: r mailto:wanghan@scut.edu.cn.

ABSTRACT

Numerous failures of fully welded flexural joints have encouraged structural designers to consider other types of alternative joints. These failure modes have been unexpected and frightening, including welded joints used to provide the optimal combination of strength, stiffness, and ductility in flexural strength frames. The research conducted in this research leads to the development of criteria for the design and use of screw fittings with an emphasis on T-Stub fittings. The primary goal is to elucidate the transmission and deformation mechanism presented in this type of connection, as well as to develop simple and reliable models for use in developing the design strategy for such connections. The ultimate goal is to provide design tools that balance the price and performance of screw joints for designers and employers. In this research, the screws were modeled in Abacus software, and by applying force, the obtained results showed that by increasing the length of the flange plate, the lever effect can be strengthened, which is effective in the tensile behavior of the screws. However, at the level of rupture performance of the web plate, the thickness of the flange plate (tf) is effective because when the screw reaches its final stress in its thread, the increase in length can lead to local rupture of the flange plate at the point of contact with the screw.

Keywords: **Sensitivity analysis, strength, modeling, high strength screws**

1. INTRODUCTION

One of the most economical ways for lateral restraint on steel frame structures is to use the steel moment-resisting frame (MRF) with fixed connections. In order to maintain the integrity of MRF buildings when subjected to horizontal forces such as wind and earthquakes, the use of bolted connections is a practical solution to provide the required restraint in the beam-column connection [1-3]. Formulating the design The beam-column connection in the frame of steel provisions to analyze the force generated in the bolts of this connection, taking into account the true behavior of the connecting components through nonlinear analysis, is a significant step in the more secure and economical design of bolt connections with the high-strength bolts, and it requires a more detailed and comprehensive examination of this issue.

structures is used to transfer the load from beam to column

[4,5]. In general, the forces transferred through the connections include the axial forces, shear forces, and torsional and flexural moments. In this study of the sensitivity analysis, the force generated in the high-strength, pre-tensioned bolts with T-stub connections is investigated. The earliest research on T-stub was conducted by Batho and Rowan (1934). In a part of the study on the riveted connections, three T-stub riveted connections were tested under uniform loads. Also, ten clip angles and three web angle connections were tested. The experiments showed that the bolted connections exhibited nonlinear moment-rotation behavior even at low load levels. In addition to providing moment-rotation curves, a method was proposed to predict the flexibility of the clip angel connection [6]. At the same time, Deng et al. in 2018, tested forty-seven connections to further examine the restraint level provided in the configurations commonly considered as the design bolted connection. A remarkable result from their study is that the slipping contact surfaces significantly contribute to the overall rotation of a bolted or riveted connection [7]. The results of Tartaglia et al. studies to estimate the strength, stiffness, and ductility of riveted connections were used in older structures. The results show that the behavior of T-stub connections is strongly influenced by the local slipping of the bolts, unreinforced panel zone yielding, and concrete encasement. It is also concluded that the use of many riveted and bolted connections throughout a structure provides a general level of stiffness compared with that of the building constructed by the slightly-welded, moment-resisting frames [8]. Putra et al. (2018) carried out three cyclic tests to compare the effects of using different types of the stiffener. All three tests were identical, except for the first one where the rivets were used. In the second and third tests, the A307 and A325 bolts were used, respectively. Contrary to popular theory, a strong punching phenomenon from the moment-rotation curve was recorded for testing the riveted connection. The punching phenomenon indicates the strong shear deformation in the rivet leading to the pre-tension loss and lower slip strength [9]. Li et al. (2017) modeled a single T element with snug-tightened bolts as a pin-ended beam with three-point loading. The forces include the T-stub web force, the bolt force, and the prying force. In addition, they considered the compatibility requirements calculated for bolt elongation [10]. This and similar views [11-14] lead to relatively long relationships, and hence, the simplified views were proposed. The application of T-stub bolted connections is one of the most widely used types of fixed bolted connections in steel structures [15-17]. The study of the change rates of the force generated in the bolts during the application of tensile loading to connections and how it changes as well as the sensitivity analysis of the force generated in the pre-tensioned bolts relative to the change in the T-stub connection geometry are among the main goals [18]. Given that the analysis of T-stub connections with pre-tensioning in the bolts (which is the most common connection in the modeling of equivalent springs) is difficult due to the complexity of the deformations in different regions, the nonlinear behavior of the materials, even in small loads, various failure modes, etc. and, on the other hand, it is costly, time-consuming and impractical for different samples to be tested, therefore, due to the quantitative and qualitative development of finite element software and their high capability to perform complex analyses, the use of various finite element software including ANSYS and ABAQUS is one of the most suitable options for researchers to study the behavior of this type of complex connections in these software [19-21]. In the vast majority of existing methods, due to the high complexity of tensile and flexural behavior of T-stub connections, their behavior analysis is usually done with some simplifications, which in some cases, make the accuracy of the results based on these analyses controversial.

2. RESEARCH METHODOLOGY

An important advantage in structural weights can be achieved by combining the limited stiffness of connections in the design and implementing the optimization method. As such, internal forces can be distributed more accurately among structural components, leading to more effective use of materials. Therefore, the cost of semi-rigid connections is generally lower compared with the fixed ones and provides an additional benefit. The bolted connections are widely used in steel frames such as MRF or simple steel component connections.

2.1. HOW TO APPLY PRE-TENSIONING FORCE IN BOLT

For the application of the pre-tensioning force in the bolt (Bolt Load), an axis to apply force to the bolt and an interior surface parallel to the cross-section of the bolt (the surface to which force is applied) are required. The datum-axis command is used to create the force axis. To create the interior surface, a datum surface or other arbitrary options could be used. The interior surface and datum axis required to apply the pre-tensioning force are shown in Figure (1).

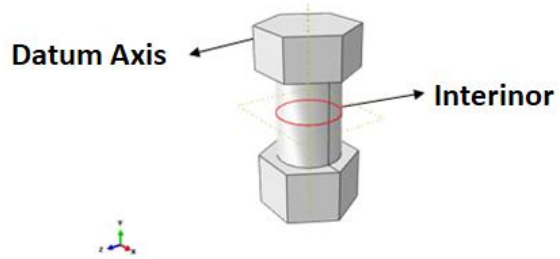

Figure 1. Interior surface and datum axis required to apply pre-tensioning force of bolt in ABAQUS software

To create the pre-tensioning force, we take the following steps:
Load module / create load / bolt load
Then, we do the following:

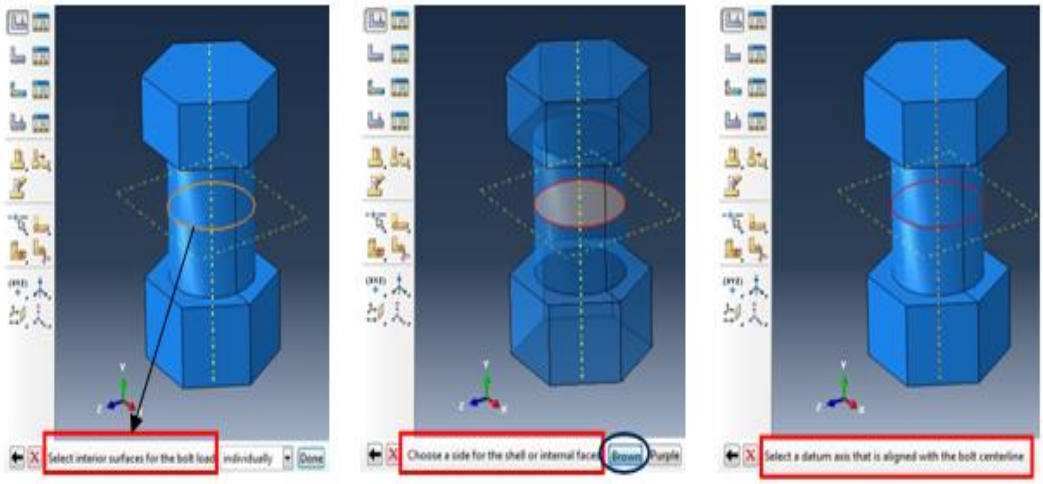

Figure 2. Settings for creating pre-tensioning force in ABAQUS software

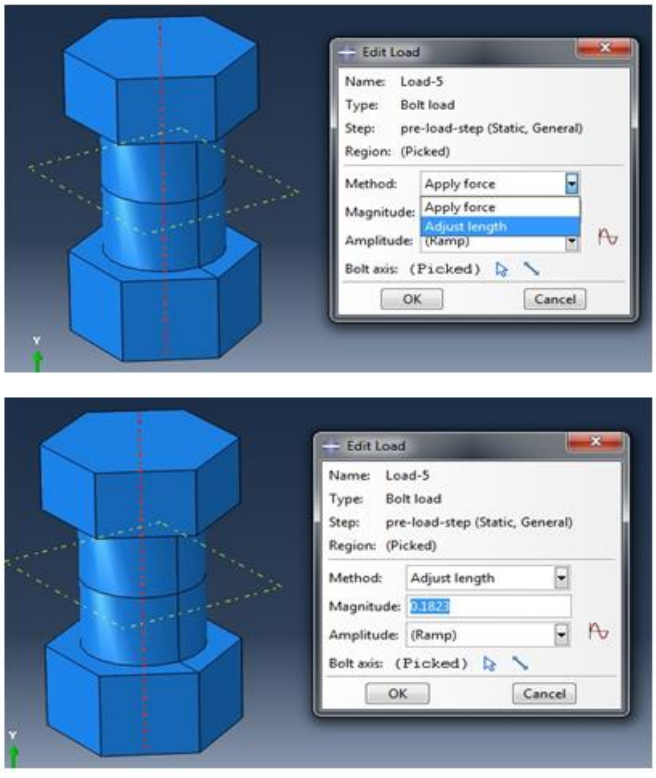

Figure 3. Settings for creating pre-tensioning force in ABAQUS software

Here, as an example, we consider how to apply the pre-tensioning force to bolt No. 24, which is 205 kN. As shown in Figure 3, in the *method* section, select *Adjust length*. In the S-1 model, the bolt must be elongated to 0.1823 mm so that the pre-tensioning force in the bolt becomes equal to 205 kN. To determine the elongation required to reach the desired force, we first consider the arbitrary elongation of 0.15mm. Then, we analyzed the model without applying the tensile force in the structure (only the pre-tensioning force of the bolt). The results show that when the 0.15mm elongation in the bolt was entered, the tensile force of the bolt reached 168.7 kN. Then, using the proportionality, we obtained the required elongation in the bolt so that the 205kN force is created in the bolt.

(205/168.7) * 0.15 = 0.1823 mm

It should be noted that when the directions of the arrows shown in the bolt cross-section are opposite, it represents the tensile force in the bolt.

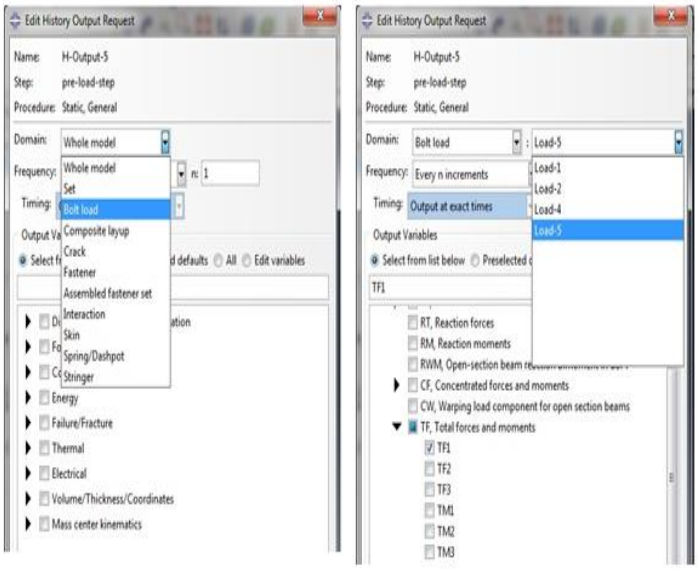

Figure 4. Settings to extract bolt force as output after analysis in ABAQUS software

After modeling the Bolt Load in the bolt, we enter the *step* module as shown in the Figure and define a *history output*. In the opened window, set *Domain* to *Bolt load* according to the left-hand table in Figure (4). Make the rest of the settings as the table on the right side of Figure (4). TF1 is the axial force in the bolt.

2.2. SAMPLES USED IN RESEARCH

In this part of the research, we introduce the samples of the statistical analysis. The samples are the same as those of T-stub connection with high-strength, pre-tensioned bolts of the previous section tested by Bursi and Jaspart (1997), which only results from the changes in its geometry. The geometric changes include the variations in the thickness of web and flange and the flange width of the T-section, the diameter of bolts, and the distance between the rows of bolts. The number of rows of bolts is one on each side. The thickness of the web is 6, 8 and 10 mm, the thickness of the flange is 10, 12, 15, 20, and 25 mm, the width of the flange is 15, 20, 25, and 30 mm, and the connection length (the length parallel to web and flange plane interface) to width ratio is 0.5, 1.0, and 1.5, and finally, the diameter of the bolts is 12, 16, 20, 24, and 27 mm. The bolts on the sides of the flange are in the middle so that the distance to each other is always half the flange width (0.5 h). The A325 bolts (according to the ISO classification) or grade 8.8 (according to ASTM) were selected with the ultimate tensile stress of 800 N/mm^2. According to Table J3-1M in AISC360-10, the pre-tensioning force of bolts of 12, 16, 20, 24 and 27mm diameter is 60.7, 91, 142, 205, and 267 kN, respectively. The bolt heads and nuts are of the hexagonal cross-section. Also, the geometry of the bolts and washers used in accordance with DIN 7990 is given in more detail in Table (1).

Table 1. Introduction of geometry details of used bolts and washers

Bolt	Washer			Nut Height (mm)	Height of Bolt Head (mm)	Diameter of Bolt Head and Nut (mm)	Real Diameter of Bolt (mm)
	Thickness (mm)	Inside Diameter (mm)	Outside Diameter (mm)				
M12	3	13	24	10	8	18	**11.3**
M16	4	17	30	13	10	24	**15.3**
M20	4	21	37	16	13	30	**19.16**
M24	4	25	44	19	15	36	**23.16**
M27	5	28	50	22	17	41	**26.16**

The number of scenarios that can be extracted from the range of variations of the above random variables is equal to 900 scenarios of T-stub connection. Obviously, not all 900 scenarios of T-stub connection are applicable. Consequently, using the Excel software environment and applying the regulation constraints, these 900 existing scenarios are reduced to fewer applicable scenarios for T-stub connection. The regulations used to comply with the design and implementation principles include the AISC360-10 and EC3 regulations. The flange width (b), flange length (h), bolt diameter (d), flange thickness (t_f), and web thickness (t_w) in the T-stub connections are considered random variables. These variables, along with the geometric configuration of the samples, are shown in Figure 5. In this section, we introduce the limitations of the regulations for choosing the applicable samples of T-stub connection from 900 possible scenarios.

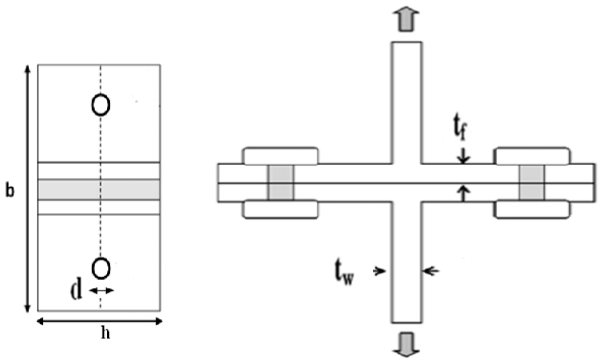

Figure 5. T-stub connection construction samples

- Minimum distance of hole centers from each other:

$$\mathbf{S_{min}} = (2\frac{2}{3})\boldsymbol{d}$$

- Minimum distance of hole centers on both side of web from each other:

$$\mathbf{S_{w,min}} = \mathbf{2(k+d)}$$

- Minimum distance of hole centers from edge:

$$\mathbf{S_{L,min}} = \begin{cases} \textbf{bolt diameter (mm)} & \mathbf{S_{L,min}(mm)} \\ \mathbf{12} & \mathbf{18} \\ \mathbf{16} & \mathbf{22} \\ \mathbf{20} & \mathbf{26} \\ \mathbf{24} & \mathbf{30} \\ \mathbf{27} & \mathbf{34} \end{cases}$$

Also, according to EC3, is equal to:

$$S_{L,min} = 1.5d$$

- Maximum distance of hole centers from each other:

$$S_{max} = min(14t_f, 200mm)$$

- Maximum distance of hole centers from edge:

$$S_{L,max} = min(12t_f, 150mm)$$

- Failure mode not to occur in T-stub web:

$$F_{t,Rd} = \sum B_{t,Rd} = \sum \frac{0.9 f_{ub} A_s}{\gamma_{Mb}}$$

$$F_{t,Sd} < F_{t,Rd}$$

$F_{t,Sd}$ = Tensile force in yielding equal to yielding capacity in web plate tension

$B_{t,Rd}$ = Design tensile strength of a bolt-plate

$\sum B_{t,Rd}$ = Total value for all bolts in T-stub connection

γ_{Mb} = Partial safety factor for connections equal to 1.25

f_{ub} = Ultimate tensile strength of bolt equal to 800 N/mm^2

A_s = Cross section of bolt under tensile stress

- Failure mode not to occur in T-stub flange:

$$t_f \leq 0.36d \sqrt{\frac{F_{ub}}{f_{yf}}}$$

F_{ub} = Ultimate tensile strength of bolt equal to 800 N/mm^2

f_{yf} = Yielding stress in T-stub flange

By controlling the constraints described above, the number of samples is reduced from 900 to 52, which is shown in Table (2) of the sample names along with their respective modified geometric details.

Table 2. Introduction of samples used in this study with modified geometric details

Sample Name	Flange Width (b) (cm)	Web Width (h) (cm)	Bolt Diameter (d) (mm)	Flange Thickness (t_f) (mm)	Web Thickness (t_w) (mm)
S-1	15	15	24	12	**6**
S-2	15	15	24	15	**6**
S-3	15	15	27	15	**6**
S-4	15	22.5	27	15	**6**
S-5	15	15	24	20	**6**
S-6	15	15	27	20	**6**
S-7	15	22.5	27	20	**6**
S-8	15	15	24	25	**6**
S-9	15	15	27	25	**6**
S-10	15	22.5	27	25	**6**
S-11	15	15	24	12	**8**
S-12	15	15	24	15	**8**
S-13	15	15	27	15	**8**
S-14	15	15	24	20	**8**
S-15	15	15	27	20	**8**
S-16	15	15	24	25	**8**
S-17	15	15	27	25	**8**
S-18	15	15	27	15	**10**
S-19	15	15	27	20	**10**
S-20	15	15	27	25	**10**
S-21	20	20	24	12	**6**
S-22	20	20	24	15	**6**
S-23	20	20	27	15	**6**

S-24	20	20	24	20	**6**
S-25	20	20	27	20	**6**
S-26	20	20	24	25	**6**
S-27	20	20	27	25	**6**
S-28	25	12.5	20	10	**6**
S-29	25	12.5	20	12	**6**
S-30	25	12.5	20	15	**6**
S-31	25	25	27	15	**6**
S-32	25	12.5	20	20	**6**
S-33	25	25	27	20	**6**
S-34	25	12.5	20	25	**6**
S-35	25	25	27	25	**6**
S-36	30	15	24	12	**6**
S-37	30	15	24	15	**6**
S-38	30	15	27	15	**6**
S-39	30	15	24	20	**6**
S-40	30	15	27	20	**6**
S-41	30	15	24	25	**6**
S-42	30	15	27	25	**6**
S-43	30	15	24	12	**8**
S-44	30	15	24	15	**8**
S-45	30	15	27	15	**8**
S-46	30	15	24	20	**8**
S-47	30	15	27	20	**8**
S-48	30	15	24	25	**8**
S-49	30	15	27	25	**8**
S-50	30	15	27	15	**10**
S-51	30	15	27	20	**10**
S-52	30	15	27	25	**10**

3. RRESULTS AND DISCUSSION

Calculation of the gradients of the response quantities obtained from the finite element analysis of the study system compared with the input parameters of the problem is required in engineering problems for various reasons. The set of such operations is called sensitivity analysis. The most important consequence of the sensitivity analysis is the introduction of indicators to measure the importance of the random variables of the system under study, which allows them to arrange these parameters in terms of the intensity affecting the behavior or response of the system, and ultimately, the reliability. To put it more formally, the sensitivity or gradient of the response is a criterion to measure the change in the system response quantities due to the application of a single change in the input parameters. One of the most advanced methods recently proposed for this purpose is the direct differentiation method (DDM), which is presented in MATLAB software. In this method, assuming that X is the vector of random and principal variables of the problem and (g_X) is a limit state function that includes the limit state functions of $g_{bolt,\ 1}$ and $g_{bolt,\ 2}$ in first and second performance levels, and also σ_X and μ_X represent the standard deviation and mean of random variables, respectively, for such case, a criterion can be defined as γ for evaluating the importance of random variables.

$$\boldsymbol{\gamma = \frac{\partial g_X}{\partial \mu_X}\sigma_X}$$

The γ-vector elements are used as a criterion for assessing the significance of each random variable in the reliability of the studied system relative to their respective In this study, the simpler concept of gradient or change increment of the limit state function relative to each of the random variables is used to determine the degree of sensitivity of the limit state function to each of the random variables. First, we differentiate the limit state function obtained from the Minitab statistical software in the MATLAB software environment relative to each random variable. In the remainder of this paper, the final differentiated functions of the limit state functions are given relative to each of the random variables $\left(\frac{\partial g_{bolt}}{\partial X_i}\right)$. In the Table, the values of the sensitivity index for each random variable are presented for the limit state functions of $g_{bolt,\ 1}$ and $g_{bolt,\ 2}$ at the first and second performance levels. These values are determined by substituting the mean value (μ_{Xi}) of each of the random variables in the final functions differentiated from the limit state functions of each of the random variables. Note that the absolute performance function. Obviously, the larger absolute values of γ elements indicate the greater importance of the corresponding variable in the behavior of that system.

values of the obtained numbers are listed in Table (3) in order to better compare the random variables with respect to the degree of sensitivity made in the limit state functions.

The final differentiated functions of the limit state function at the first performance level:

$$\frac{\partial g}{\partial b} = -\frac{11}{25} + \frac{231}{50000} \times b + \frac{1}{40} \times d + \frac{533}{1000} \times t_w - \frac{17}{125} \times t_f - \frac{5238875316933513}{18446744073709551616} \times h \times t_f - \frac{2960702423830383}{4611686018427387904} \times b \times t_f + \frac{103}{25000} \times d \times t_f - \frac{147}{10000} \times d \times t_w + \frac{841}{100000} \times {t_f}^2 - \frac{789}{50000} \times t_f \times t_w + \frac{37}{5000} \times {t_w}^2$$

$$\frac{\partial g}{\partial h} = -\frac{583}{100} - \frac{87}{5000} \times h + \frac{81}{500} \times t_f - \frac{11}{40} \times d - \frac{5238875316933513}{18446744073709551616} \times b \times t_f + \frac{6622381122461729}{4611686018427387904} \times h \times t_f - \frac{99}{10000} \times d \times t_f - \frac{1}{400} \times {t_f}^2$$

$$\frac{\partial g}{\partial d} = 80 - \frac{15446}{3125} \times d + \frac{1}{40} \times b - \frac{13}{10} \times t_f + \frac{323}{50} \times t_w - \frac{11}{40} \times h + \frac{103}{25000} \times b \times t_f - \frac{147}{10000} \times b \times t_w - \frac{99}{10000} \times h \times t_f + \frac{37}{625} \times {t_f}^2 - \frac{1}{10} \times t_f \times t_w$$

$$\frac{\partial g}{\partial t_f} = \frac{261}{10} + \frac{81}{500} \times h - \frac{13}{10} \times d + \frac{16}{25} \times t_f - \frac{17}{125} \times b - \frac{181}{100} \times t_w - \frac{567}{2500} \times {t_f}^2 - \frac{5238875316933513}{18446744073709551616} \times b \times h - \frac{2960702423830383}{9223372036854775808} \times {b}^2 + \frac{103}{25000} \times b \times d + \frac{841}{50000} \times b \times t_f - \frac{789}{50000} \times b \times t_w + \frac{6622381122461729}{9223372036854775808} \times {h}^2 - \frac{99}{10000} \times h \times d - \frac{1}{200} \times h \times t_f + \frac{74}{625} \times d \times t_f - \frac{1}{10} \times d \times t_w + \frac{407}{1000} \times t_f \times t_w - \frac{19}{1000} \times {t_w}^2$$

$$\frac{\partial g}{\partial t_w} = -127 + \frac{533}{1000} \times b + \frac{323}{50} \times d - \frac{121}{25} \times t_w - \frac{181}{100} \times t_f - \frac{147}{10000} \times b \times d - \frac{789}{50000} \times b \times t_f + \frac{37}{2500} \times b \times t_w - \frac{1}{10} \times d \times t_f + \frac{407}{2000} \times {t_f}^2 - \frac{19}{500} \times t_f \times t_w$$

The final differentiated functions of the limit state function at the second performance level:

$$\frac{\partial g}{\partial b} = -\frac{177}{20} - \frac{2339}{100000} \times t_f \times t_w - \frac{3}{125} \times t_f + \frac{817}{1000} \times t_w + \frac{701}{25000} \times b + \frac{59}{500} \times d - \frac{1046852726183017}{1152921504606846976} \times b \times t_f + \frac{2600990914393047}{18446744073709551616} \times h \times t_f + \frac{31}{25000} \times d \times t_f + \frac{793}{100000} \times {t_f}^2 + \frac{39}{2500} \times {t_w}^2$$

$$\frac{\partial g}{\partial h} = -\frac{2}{25} + \frac{711}{50000} \times h - \frac{6}{125} \times t_f - \frac{33}{500} \times d + \frac{2600990914393047}{18446744073709551616} \times b \times t_f - \frac{7055879608193903}{4611686018427387904} \times h \times t_f + \frac{57}{10000} \times d \times t_f + \frac{197}{50000} \times {t_f}^2$$

$$\frac{\partial g}{\partial d} = -59 + \frac{829}{250} \times d + \frac{59}{500} \times b - \frac{309}{100} \times t_f + \frac{73}{20} \times t_w - \frac{33}{500} \times h + \frac{31}{25000} \times b \times t_f - \frac{27}{1250} \times b \times t_w + \frac{57}{10000} \times h \times t_f + \frac{81}{2500} \times {t_f}^2 + \frac{8}{125} \times t_f \times t_w$$

$$\frac{\partial g}{\partial t_f} = \frac{51}{2} - \frac{6}{125} \times h - \frac{309}{100} \times d + \frac{557}{500} \times t_f - \frac{3}{125} \times b + \frac{249}{100} \times t_w - \frac{1659}{10000} \times {t_f}^2 + \frac{2600990914393047}{18446744073709551616} \times b \times h - \frac{1046852726183017}{2305843009213693952} \times {b}^2 + \frac{31}{25000} \times b \times d + \frac{793}{50000} \times b \times t_f - \frac{2339}{100000} \times b \times t_w - \frac{7055879608193903}{9223372036854775808} \times {h}^2 + \frac{57}{10000} \times h \times d + \frac{197}{25000} \times h \times t_f + \frac{81}{1250} \times d \times t_f + \frac{8}{125} \times d \times t_w - \frac{1}{1000} \times t_f \times t_w + \frac{39}{1000} \times {t_w}^2$$

$$\frac{\partial g}{\partial t_w} = -\frac{1593}{10} + \frac{817}{1000} \times b + \frac{73}{20} \times d - \frac{383}{50} \times t_w - \frac{181}{100} \times t_f - \frac{27}{1250} \times b \times d - \frac{2339}{100000} \times b \times t_f + \frac{39}{1250} \times b \times t_w + \frac{8}{125} \times d \times t_f - \frac{1}{2000} \times {t_f}^2 + \frac{39}{500} \times t_f \times t_w$$

Table 3. Sensitivity of limit state function (g_{bolt}) to random variables

$(\frac{\partial g_{bolt}}{\partial X_i})$		
X_i	Performance Level	
	First (web plate yielding)	Second (web plate failure)
b	2.607	0.239
h	14.123	0.401
d	87.392	118.803
t_f	4.994	3.167
t_w	181.506	208.074

As can be seen in the above table, the order from the maximum to minimum of the importance or sensitivity of the random variables on the limit state function (g_{bolt}) relative to the random variables at the first performance level or the yielding of the T-stub web plate is the thickness of web plate (t_w), bolt diameter (d), length of flange plate (h), the thickness of flange plate (t_f) and width of flange plate (b). Also, at the second performance level or the web plate failure of the T-stub connection, respectively, they are the thickness of web plate (t_w), bolt diameter (d), the thickness of flange plate (t_f), length of the flange plate (h) and width flange plate (b).

As already predicted, the random variable of web plate thickness (t_w) at both performance levels has the highest importance or sensitivity for the limit state function (g_{bolt}) among other random variables with a significant percentage. The most important reason for this can be attributed to the determining factor of web plate thickness of T-stub connection in the ultimate strength for different performance levels so that for the known thickness of web plate (t_w) along with a given width of web plate (b), the allowable tensile strength resisted by the bolts for each performance level is determined. For example, in this study, the ultimate strength function of the bolts at the first performance level is equal to the yielding force of the web plate, and at the second performance level, it is equal to the failure force of the web plate. Hence, by determining the thickness of the web plate (t_w), the acceptable bolt number (diameter required for bolts) is obtained. The next order of the random variables in terms of importance or sensitivity to the limit state function (g_{bolt}) is the bolt diameter (d) that is more sensitive to the remaining random variables. The bolt diameter determines the pre-tensioning force in accordance with the regulations, and hence, the selection of bolt diameter is equivalent to determining the initial conditions for T-stub connection in terms of tensile strength. Because the tensile capacity of the bolts is increased by applying the pre-tensioning force to the bolts, by which as the tensile strength continues to apply to the T-stub connection, the behavior of the bolts becomes completely different. Therefore, the random variables of the bolt diameter (d) after the random variable of the web plate thickness (t_w) have a high sensitivity to the behavior of the high-strength, pre-tensioned bolts relative to the remaining random variables. The third most important random variable is different based on the behavior of the high-strength, pre-tensioned bolts in the T-stub connection for the first and second performance levels. In the first performance level or the yielding of the web plate, it is the length flange plate (h), because once the web plate is yielded, the prying action could be intensified by increasing the length of the flange plate, which affects the tensile behavior of the bolts. But in the second performance level or failure of web plate, the thickness of the flange plate (t_f) is the third most important random variable on the limit state function (g_{bolt}), since, when the bolt thread reaches its ultimate stress level (second performance level), due to large non-elastic deformations, the length could be increased which can lead to the local failure of the flange plate as the pinching or rupture in contact with the bolt. That is why the thickness of the flange plate is more sensitive than the width and length of the flange plate because as the thickness of the flange plate is increased, the failure mode of the bolts could be delayed, which improves the behavior of high-strength bolts in T-stub connections. The two remaining random variables, which have the least importance on the behavior of the bolts, or the limit state function (g_{bolt}) at the first performance level, are the width of the flange plate (b) and the thickness of the flange plate (t_f). These two variables are almost identical with a significant distance to other random variables in terms of the effect on the limit state function (g_{bolt}), since, when the main body of bolt reaches its yielding limit (first performance level), it experiences small elastic deformation, which is insignificant relative to the deformation occurring in the connection flange so that the thickness and width of the flange plate have the least effect on whether the bolts are yielded or not. However, the two remaining random variables in terms of significance in the behavior of the bolts, or the limit state function (g_{bolt}) at the second performance level, are the length of flange plate (h) and width of flange plate (b), which significantly differ from the other random variables, they can cause almost identical and insignificant sensitivity. Because at the moment when the high-strength, pre-tensioned bolts in the T-stub connection reach their

ultimate limit (second performance level), they undergo a large axial deformation, and the only effective parameter of the flange plate to delay this failure mode in the bolts is the thickness of flange plate that can reduce or increase the strength of the flange plate against large non-elastic bolt deformations by decreasing or increasing it.

4. CONCLUSION

In this paper, the sensitivity analysis of the force generated in the high-strength, pre-tensioned bolts with T-stub connections was investigated.

- The random variable of web plate thickness (t_w) at both performance levels has the highest sensitivity for the limit state function (g_{bolt}) among other random variables with a significant percentage. The most important reason for this can be attributed to the determining factor of web plate thickness of T-stub connection in the ultimate strength for different performance levels so that for the known thickness of web plate (t_w) along with a given width of web plate (b), the allowable tensile strength resisted by the bolts for each performance level is determined.
- The second random variable in terms of sensitivity to the limit state function (g_{bolt}) is the bolt diameter (d), which is more sensitive to the remaining random variables. The bolt diameter determines the pre-tensioning force in accordance with the regulations, and hence, the selection of bolt diameter is equivalent to determining the initial conditions for T-stub connection in terms of tensile strength. Because the tensile capacity of the bolts is increased by applying the pre-tensioning force to the bolts by which, as the tensile strength continues to apply to the T-stub connection, the behavior of the bolts becomes completely different.
- The third most important random variable is different for the first and second performance levels. In the first performance level, the yielding of the web plate is the length flange plate (h) because once the web plate is yielded, the prying action could be intensified by increasing the length of the flange plate, which affects the tensile behavior of the bolts. But in the second performance level, failure of web plate, it is the thickness of flange plate (t_f), since, when the bolt thread reaches its ultimate stress level (second performance level), due to large non-elastic deformations, the length could be increased which can lead to the local failure of the flange plate as the pinching or rupture in contact with the bolt.

FUNDING/SUPPORT

Not mentioned any Funding/Support by authors.

ACKNOWLEDGMENT

Not mentioned by authors.

AUTHORS CONTRIBUTION

This work was carried out in collaboration among all authors.

CONFLICT OF INTEREST

The author (s) declared no potential conflicts of interests with respect to the authorship and/or publication of this paper.

5. REFERENCES

[1] Mehmanparast A, Lotfian S, Vipin SP. A review of challenges and opportunities associated with bolted flange connections in the offshore wind industry. Metals. 2020 Jun;10(6):732. [View at Google Scholar]; [View at Publisher].

[2] Elliott MD, Teh LH, Ahmed A. Behaviour and strength of bolted connections failing in shear. Journal of constructional steel research. 2019 Feb 1;153:320-9. [View at Google Scholar]; [View at Publisher].

[3] Redondo R, Mehmanparast A. Numerical analysis of stress distribution in offshore wind turbine M72 bolted connections. Metals. 2020 May;10(5):689. [View at Google Scholar]; [View at Publisher].

[4] Chen Z, Niu X, Liu J, Khan K, Liu Y. Seismic study on an innovative fully-bolted beam-column joint in prefabricated modular steel buildings. Engineering Structures. 2021 May 1;234:111875. [View at Google Scholar]; [View at Publisher].

[5] Jiang ZQ, Chen ML, Yang ZS, Li XY, Cai C. Cyclic loading tests of self-centering prestressed prefabricated steel beam-column joint with weakened FCP. Engineering Structures. 2022 Feb 1;252:113578. [View at Google Scholar]; [View at Publisher].

[6] Batho C, Rowan HC. Investigations on beam and stanchion connections. Second Report of the Steel Structures Research Committee. London. 1934 May. [View at Google Scholar];

[7] Deng Etal, Zong L, Ding Y, Luo YB. Seismic behavior and design of cruciform bolted module-to-module connection with various reinforcing details. Thin-Walled Structures. 2018 Dec 1;133:106-19. [View at Google Scholar]; [View at Publisher].

[8] Tartaglia R, D'Aniello M, Zimbru M. Experimental and numerical study on the T-Stub behaviour with preloaded bolts under large deformations. InStructures 2020 Oct 1 (Vol. 27, pp. 2137-2155). Elsevier. [View at Google Scholar]; [View at Publisher].

[9] Putra GL, Kitamura M, Takezawa A. Structural optimization of stiffener layout for stiffened plate using hybrid GA. International Journal of Naval Architecture and Ocean Engineering. 2019 Jul 1;11(2):809-18. [View at Google Scholar]; [View at Publisher].

[10] Li G, Fang Y, Hao P, Li Z. Three-point bending deflection and failure mechanism map of sandwich beams with second-order hierarchical corrugated truss core. Journal of Sandwich Structures & Materials. 2017 Jan;19(1):83-107. [View at Google Scholar]; [View at Publisher].

[11] Monteiro AC, Malite M. Behavior and design of concentric and eccentrically loaded pultruded GFRP angle columns. Thin-Walled Structures. 2021 Apr 1;161:107428. [View at Google Scholar]; [View at Publisher].

[12] Meng X, Gardner L. Cross-sectional behaviour of cold-formed high strength steel circular hollow sections. Thin-Walled Structures. 2020 Nov 1;156:106822. [View at Google Scholar]; [View at Publisher].

[13] Camotim D, Martins AD, Dinis PB, Young B, Chen MT, Landesmann A. Mode interaction in cold-formed steel members: state-of-art report: Part 1: Fundamentals and local-distortional coupling. Steel Construction. 2020 Aug;13(3):165-85. [View at Google Scholar]; [View at Publisher].

[14] Bompa DV, Elghazouli AY. Behaviour of confined rubberised concrete members under combined loading conditions. Magazine of Concrete Research. 2021 Jun;73(11):555-73. [View at Google Scholar]; [View at Publisher].

15] Gödrich L, Wald F, Kabeláč J, Kuříková M. Design finite element model of a bolted T-stub connection component. Journal of Constructional Steel Research. 2019 Jun 1;157:198-206. [View at Google Scholar]; [View at Publisher].

[16] Wang P, Sun L, Zhang B, Yang X, Liu F, Han Z. Experimental studies on T-stub to hollow section column connection bolted by T-head square-neck one-side bolts under tension. Journal of Constructional Steel Research. 2021 Mar 1;178:106493. [View at Google Scholar]; [View at Publisher].

[17] Bezerra LM, Bonilla J, Freitas CS, Massicotte B. Behavior of T-stub steel connections bolted to rigid bases. Journal of Constructional Steel Research. 2022 May 1;192:107242. [View at Google Scholar]; [View at Publisher].

[15] Yuan HX, Hu S, Du XX, Yang L, Cheng XY, Theofanous M. Experimental behaviour of stainless steel bolted T-stub connections under monotonic loading. Journal of Constructional Steel Research. 2019 Jan 1;152:213-24. [View at Google Scholar]; [View at Publisher].

[18] Kong Z, Kim SE. Numerical estimation for initial stiffness and ultimate moment of T-stub connections. Journal of Constructional Steel Research. 2018 Feb 1;141:118-31. [View at Google Scholar]; [View at Publisher].

[19] Zhang Y, Gao S, Guo L, Fu F, Wang S. Ultimate tensile behavior of bolted stiffened T-stub connections in progressive collapse resistance. Journal of Constructional Steel Research. 2022 Feb 1;189:107111. [View at Google Scholar]; [View at Publisher].

[20] Baldassino N, Bernardi M, Zandonini R. Experimental and numerical study of the loading rate influence on T-stub performance. InAIP Conference Proceedings 2022 Apr 6 (Vol. 2425, No. 1, p. 120013). AIP Publishing LLC. [View at Google Scholar]; [View at Publisher].

[21] Gao F, Liu Z, Guan X. Fire resistance behavior of T-stub joint components under transient heat transfer conditions. Engineering Structures. 2021 Jun 15;237:112164. [View at Google Scholar]; [View at Publisher].